Available online at www.sciencedirect.com
ScienceDirect
European Journal of Pharmaceutics and Biopharmaceutics 65 (2007) 270–281
European Journal of Pharmaceutics and Biopharmaceutics
www.elsevier.com/locate/ejpb

Review article

Fate of micelles and quantum dots in cells

Dusica Maysinger [a,*], Jasmina Lovrić [a,b], Adi Eisenberg [c], Radoslav Savić [a]

[a] Department of Pharmacology and Therapeutics, McGill University, Montreal, Canada
[b] Department of Pharmaceutical Technology, University of Zagreb, Zagreb, Croatia
[c] Chemistry Department, McGill University, Montreal, Canada

Received 27 June 2006; accepted in revised form 17 August 2006
Available online 1 September 2006

Abstract

Micelles and quantum dots have been used as experimental drug delivery systems and imaging tools both in vitro and in vivo. Investigations of their fate at the subcellular level require different surface-core modifications. Among the most common modifications are those with fluorescent probes, dense-core metals or radionucleids. Cellular fate of several fluorescent probes incorporated into poly(caprolactone)-b-copolymer micelles (PCL-b-PEO) was followed by confocal microscopy, and colloidal gold incorporated in poly 4-vinyl pyridine-PEO micelles were developed to explore micelle fate by electron microscopy. More recently, we have examined quantum dots (QDs) as the next-generation-labels for cells and nanoparticulate drug carriers amenable both to confocal and electron microscopic analyses. Effects of QDs at the cellular and subcellular levels and their integrity were studied. Results from different studies suggest that size, charge and surface manipulations of QDs may play a role in their subcellular distribution. Examples of pharmacological agents incorporated into block copolymer micelles, administered or attached to QD surfaces show how the final biological outcome (e.g. cell death, proliferation or differentiation) depends on physical properties of these nanoparticles.

Keywords: Block copolymer micelles; Quantum dots; Internalization; Stability; Confocal microscopy; Multiple labeling; Fluorescent dyes; Organelles

1. Block copolymer micelles

1.1. Definition and properties

Block copolymer micelles are nanosized (10–100 nm) particles dispersed in water. They are prepared from synthetic polymers that contain hydrophilic and hydrophobic parts. The hydrophilic part is commonly poly(ethylene oxide), PEO, and the hydrophobic part is varied from amino acids, polyesters and poloxamers [1]. PEO is usually used to decrease contact between macromolecules in the surrounding environment and surfaces coated with PEO. The molecular mass of PEO blocks [2] and surface density [3] must be tailored to achieve the protein repelling effect. Presence of PEO in the outer shell (exposed to the surrounding environment) of block copolymer micelles contributes to maintaining the micelles dispersed in solution and hinders their contact with cells [4]. The most commonly investigated micelles are of spherical shape. However, various morphologies are attainable, and transition between micelles and vesicles [5] by varying the solution properties is well documented [6,7]. To create spherical micelles the hydrophilic part of the polymer should not outweigh the hydrophobic portion [8]. The characteristic feature of block copolymer micelles is their core-shell structure (Fig. 1).

The core is comprised of hydrophobic parts of the polymer, and its physical state can vary from swollen to frozen depending on the glass transition temperature (T_g) of the polymer. The defining properties of micelles include critical micellar concentration (CMC), aggregation number, size and shape [9]. The size of micelles allows their selective accumulation in sites with leaky vasculature, through enhanced permeability and retention effect [10,11].

* Corresponding author. Department of Pharmacology and Therapeutics, McGill University, 3655 Promenade Sir William Osler, Montreal, Que., Canada H3G 1Y6. Tel.: +1 514 3981264; fax: +1 514 3986690.
E-mail address: dusica.maysinger@mcgill.ca (D. Maysinger).

0939-6411/$ - see front matter © 2006 Elsevier B.V. All rights reserved.
doi:10.1016/j.ejpb.2006.08.011

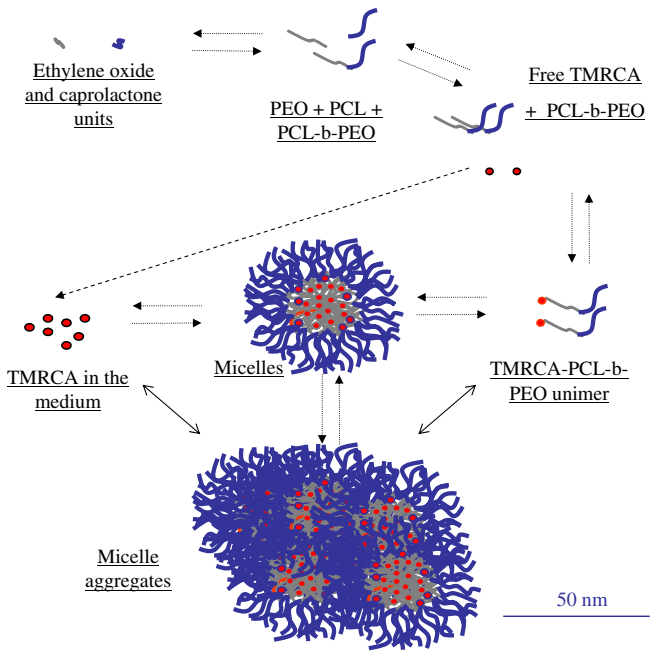

Fig. 1. Micelle dynamics and stability. PCL-b-PEO micelles are dynamic systems which accommodate lipophilic agents (e.g. drugs and fluorescent dyes such as TMRCA) in their hydrophobic PCL cores. The hydrophilic PEO parts form corona that separate core from aquatic environment. Multiple equilibria exist between micelles and their components, i.e. entrapped agents (TMRCA) and PCL-b-PEO unimers. Under physiological conditions micelles can form large aggregates.

1.2. Micelles as drug delivery vehicles

The purpose of using block copolymer micelles in medical sciences is to minimize the hydrophobic drugs of solubility problems, toxicity and inadequate pharmacokinetics. The most significant advances were made with anticancer agents and these delivery systems have recently reached clinical trials [12–14]. Steroid hormones can be also very effectively incorporated into block-copolymer micelles [15,16]. Such micelles could provide drug-loaded depot systems with controllable release that could find use in hormone replacement therapy. Immunosuppressant agent FK506, incorporated into PCL-b-PEO micelles administered at the site of sciatic nerve lesion, can facilitate repair of the peripheral nerves [17]. Micelles seem to be suitable nanocarriers for a number of anti-inflammatory agents, and the local delivery of anti-inflammatory drugs through accumulation of micelles effectively reduces vascular leakage at inflamed sites [18–20]. Block copolymer micelles made of charged block copolymers have been investigated for non-viral delivery of genetic material [21,22] and other charged molecules [23]. The self-assembly of polyion complex micelles (PICM) proceeds through the neutralization and segregation of oppositely charged polyions in a way that combines features of amphiphilic micelles and interpolyelectrolyte complexes. Polymers having protonated amines at physiological pH may be considered good candidates for the preparation of PICM incorporating polyanionic molecules such as plasmid DNA [24], oligonucleotides [25] and enzymes [26]. Examples of such polymers are poly(ethyleneimine) (PEI), PLys, polyamidoamide and poly(2-(*N*,*N*-dimethylamino)ethyl methacrylate) [27]. However, some of these polymers are cytotoxic (e.g. PEI). In order to form PICM with polycationic drugs, polymers exhibiting negatively charged units, including poly(methacrylic acid) and PAsp, are required [28]. Properties and application of ionomers forming micelles have been recently reviewed [23].

1.3. Selected approaches to labeling the micelles

The cellular fate of block copolymer micelles is relevant for evaluating and optimizing the delivery system. The distribution of micelles inside living cells can be followed by fluorescent labeling of the constitutive block copolymers. For example, red fluorescent dyes [29], green fluorescent dyes [30] and drugs [31] have been covalently coupled to the polymer and fate of the micelles investigated by confocal microscopy. Combined with the use of organelle selective dyes (Table 1) the details of the cellular distribution of micelles in live cells were assessed [32] (Fig. 2). Alternatively block copolymers can be labeled with radioactive probes [16,17,33–35], and heavy atoms such as gold [36,37], so that they can be revealed by electron microscopy. Gold, because of its high electron density and stability, can be incorporated into micelles to allow visualization of individual micelles by TEM. This technique provides information on intracellular location of gold-associated particles with much better resolution than is achievable by optical microscopy. To date, however, there are no TEM reports showing the presence of individual micelles in subcellular compartments, although many groups have investigated the association between heavy metals and polymers for various applications [38–43]. We have prepared and characterized gold-incorporated micelles [36]. Such micelles can enter the cells when incubated for at least one hour and can be seen as agglomerates by TEM (Fig. 2). Similar to the findings with fluorescent-labeled micelles, the data suggest that the micelles do not enter the nucleus but they can be found in endosomes/lysosomes. Although this approach cannot be used to study the fate of micelles in real time [44], it has the advantage of providing more refined information on subcellular distribution within cell organelles (Fig. 2).

In summary, using both fluorescently labeled agents and fluorescent polymers we were able to distinguish between micelle-incorporated agents and unlabeled micelles and to provide the evidence for their intracellular location. The most compelling evidence for internalized micelles containing fluorescent agents was obtained by fluorescence lifetime imaging (FLIM) [45–47]. The principle of the FLIM experiments consists of the following steps: (i) the life-time of the donor fluorescence is measured in the absence of an acceptor fluorophore (control); (ii) another sample is prepared where both donor and acceptor fluorophores are present and both are imaged by confocal microscope; (iii) FLIM instrument measures the lifetime of the donor fluo-

Table 1
Organelle markers used for micelle (QD) subcellular localization

Compartment	"Marker"	Comment	Reference
Plasma membrane	DAF	The lipophilic fluorescein probes	[32]
	DiI	Carbocyanine lipophilic probes	www.probes.com
	GFP-F	Farnesylated GFP	Clontech www.clotech.com
Clathrin-coated pits	Clathrin-DsRed	Live cell imaging of protein recruitment to clathrin-coated pits	[51]
	Transferrin conjugates	For tracking receptor-mediated endocytic processes	www.probes.com
Early endosomes	Dextran conjugates	For tracking uptake of exogenous material by phagocytosis and endocytosis	www.probes.com
	EEA1	Immunolabeling of early endosome antigen 1	[52]
Lysosomes	LysoTrackers	Fluorescent acidotropic probes for labeling of acidic organelles	[32] www.probes.com
Phagosomes	GFP-Rab 5,7	For tracing early and late endo/phagocytic compartments	[53]
	Latex beads	Phagocytosed particles with defined size ranges	www.probes.com
Caveolae	Bodipy-LacCer	Sphingolipid internalized almost exclusively through caveolae-mediated pathway	[54]
ER	ER Tracker blue-white	Non-toxic ER selective dye for live cell imaging	[55] www.probes.com
Golgi apparatus and ER	Brefeldin A BODIPY® FL conjugate	Selectively localized in Golgi apparatus and ER	www.probes.com
Mitochondria	MitoTrackers	Accumulate in active mitochondria	[32] www.probes.com
Cytoskeleton	Actin-Phalloidin	Phallotoxin derivatives that selectively stain F-actin	[56] www.probes.com
Nucleus	Hoechst	The minor groove binding, dsDNA selective dye for live cell imaging	www.probes.com
	DAPI	Classic nucleic acid stain for fixed cells	

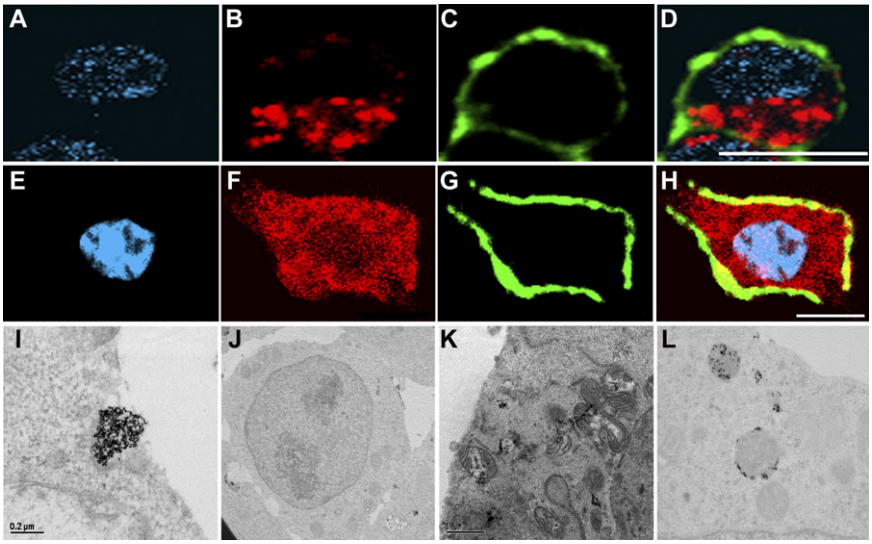

Fig. 2. Subcellular distribution of micelles. Cytoplasmic distribution of fluorescent-labeled PCL-b-PEO micelles (A–D) and diffuse distribution of the free TMRCA label (E–H) is revealed by confocal microscopy. Gold-labeled PCL-b-PEO micelles aggregate in the cell culture medium and as such interact with cell surface (I). Gold-labeled micelles do not enter nuclei (J) and only a few can be found in mitochondria (K). Most of the gold-labeled micelles are found in endosomes/lysosomes (L) as revealed by electron microscopy.

rophore when the acceptor is present. If the lifetime of the donor is shortened, it implies FRET, and a close proximity between the two fluorophores. Combining FLIM with FRET provides high spatial resolution in the intact cells. We studied interactions between red micelle-incorporated or red free dye and green dye inserted into plasma membranes. The free red dye (tetramethylrhodamine-5-carbonyl azide TMRCA, acceptor) undergoes FRET interactions with the green membrane dye (5-dodecanoylaminofluorescein, DAF, donor) in the absence of micelles (Fig. 3). As a result of this interaction there is a decrease in life-time of the donor dye DAF from approximately 2400 to 1700 ps. In contrast, no FRET interactions are seen when TMRCA is incorporated into micelles since the distance between the donor and acceptor dye is too large (>10 nm).

Although, fluorescent dyes are useful for tracking micelles they have several limitations, particularly if time-lapse experiments are required or if multiple laser exposures

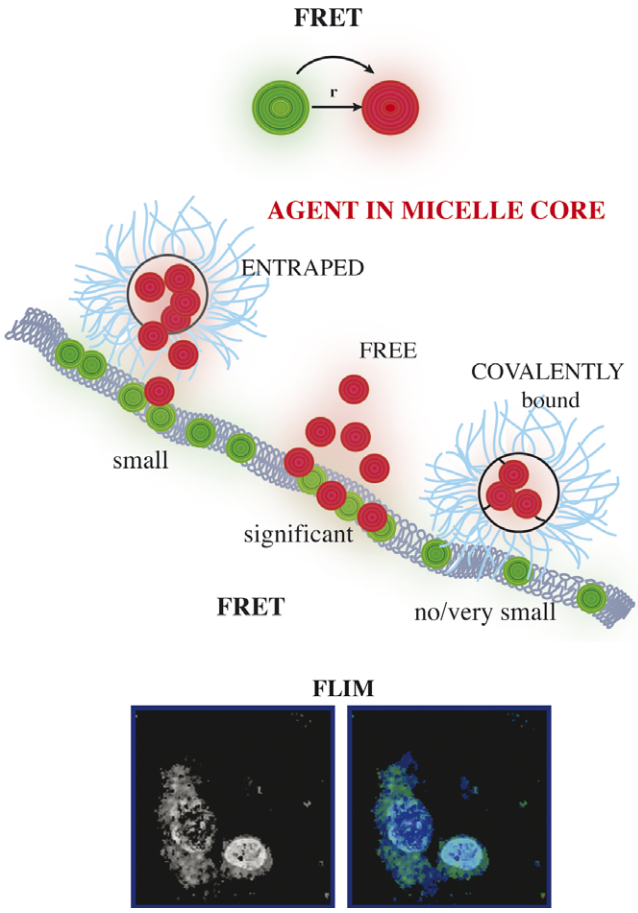

Fig. 3. Fluorescence resonance energy transfer (FRET) between the fluorescent agents. FRET is a proximity-based assay which provides information about close proximity of two fluorescent agents. It occurs when the distance between a green (e.g. membrane) and red fluorescing dye (TMRCA) is very small. FRET is absent between the green and red emitting-dye if micelles contain fluorescent label covalently bound within the micelle core because the distance between the incorporated agent (red) and the green dye-labeled membrane is too big. This is confirmed by fluorescence life-time imaging (FLIM) where the absence of energy transfer and lack of change in half-life are shown as different intensities of blue. (For interpretation of the references to color in this figure legend, the reader is referred to the web version of this paper.)

are needed. QDs (discussed later in this article) represent an interesting novel alternative labeling strategy to follow the fate of micelles by confocal and electron microscopy [48–50].

1.4. Selected molecular manipulations to study the internalization of micelles

The internalization of block copolymer micelles involves endocytosis [29,30]. Endocytotic pathways involve pinocytosis, caveolae, clathrin, and caveolae-clathrin independent processes [57,58]. The best characterized pathway is clathrin-dependent endocytosis [59] involving a number of accessory factors (Table 2). Specific information about the internalization of block copolymer micelles could be obtained by regulation of specific proteins and their phosphorylation status. Among the approaches used to explore nanoparticles and macromolecule endocytosis are genetic mutations (Table 2) and pharmacological manipulations (Table 3).

1.5. Micelle stability

Physical stability of nanoparticles is a fundamental requirement for an effective drug delivery system. In contrast to low molecular mass surfactants, polymeric micelles exhibit significantly lower values for critical association constant (CAC), indicating greater thermodynamic stability than naturally occurring micelles. The rate at which the micelles tend to dissociate is related to their composition, their physical state and the cohesion of the micelle core. Micellar stability correlates well with the length of the hydrophobic segment in the amphiphilic copolymer, with higher proportions of hydrophobic polymer conferring greater thermodynamic stability [23]. Gaucher et al. have demonstrated by a steady-state pyrene fluorescence technique that increasing the PDLLA proportion in PVP-b-PDLLA-b-PVP triblock copolymers from 27 to 55 mol % led to a significant decrease in the CAC values [23]. Jette et al. showed that an increase in the length of the core-forming segment could reduce fenofibrate leakage while enhancing the resistance of PEG-b-PCL polymeric micelles towards dissociation [78]. Among several PEG-b-poly(alkylmethacrylate)s with identical degrees of polymerization but with monomers of different degrees of hydrophobicity, the lowest CAC was achieved for the most hydrophobic copolymer [79]. Other groups have focused on modifying the properties of the core-forming blocks in an attempt to enhance their hydrophobicity [80–82]. Cross-linking of the shell or core of hydrophobic micelles is a promising strategy to increase the micelle stability [83]. Shuai et al. performed the core cross-linking of paclitaxel-loaded PEG-b-PCL micelles by radical polymerization of double bonds introduced into the PCL blocks. These micelles exhibited significantly enhanced stability against dilution with aqueous solvents, i.e. no collapse of micelles was detected upon dilution (1000×), as determined by dynamic light scattering and gel permeation chromatography [84]. More recently, Kataoka prepared remarkably stable trypsin-loaded PEG-b-P(Asp) PICM cross-linked using glutaraldehyde without loss of protein activity [85]. Strong cohesive forces between the drug and the polymer core segments also play a role in micelle stability as shown by Lee et al. [86].

CAC values of PEG-b-PLys carrying antisense ODN determined by Kataoka's group were found to be around 140–170 mg/L [87]. These values are superior to the CAC of most amphiphilic copolymer micelles and suggest that dissociation of PICM upon dilution could seriously compromise their in vivo performance.

Recent studies by Savić et al. demonstrated marked differences in PCL-b-PEO micelle stability depending on the microenvironment [88]. Fluorogenic dye incorporated into

Table 2
Molecular mutations of endogenous proteins to study nanoparticle entry

Protein	Effect	Comment	Reference
Dynamin mutant	Prevents the calveolae- and raft-mediated internalization of various molecules	Blocks early events in endocytosis	[60]
AP180	Impairs the efficiency of synaptic vesicle endocytosis and alters the normal localization of clathrin	APs sequester membrane cargo into developing clathrin-coated pits	[61]
Eps 15	The plasma membrane punctuated distribution of both AP-2 and clathrin was lost, implying the absence of coated pits	It plays an important role in the docking of AP2 to plasma membrane during coated pit assembly	[62]
Rab mutants	Mutations of RAB5 and RAB7 are associated with early and late endocytosis, respectively	Rab family of proteins is essential for the regulation of intracellular membrane traffic	[63,64]
Arf mutants	Mutation of Arf6 has pronounced effect on receptor-mediated endocytic trafficking	Arf GTPases are required for maintaining the organelle structure and intracellular trafficking	[65]
Rho-GTPase mutants	Overexpression of constitutively active forms of Rac1 or RhoA inhibits receptor-mediated endocytosis	Rho-GTPases are critical regulators of many stages of vesicular trafficking	[66,67]
Intersectin	Expression of Dbl- domain constructs induces actin rearrangements specific for Cdc42 (Rho-GTPase) activation	Scaffolding protein that regulates the formation of clathrin-coated pits and caveolae	[68]
Caveolin-1	Targeted disruption of caveolin-1 leads to the loss of the caveolae	Cholesterol-binding integral membrane protein essential for the formation of caveolae	[69]

Table 3
Pharmacological inhibitors of nanoparticle entry

Agent	Effect	Reference
Nocodazole	Promotes tubulin depolymerization	[70]
Lantrunculin A	Sequesters actin monomers, blocks actin polymerization and promotes actin depolymerization	[71]
Monensin	Disruption of lysosome and endosome function	[72,73]
Brefeldin A	Causes disassembly of the Golgi complex and ER swelling	[74]
Cytochalasin D	Inhibits actin polymerization and interferes with microtubule assembly by reacting with sulfhydryl groups	[70]
Bafilomycin	Blocks lysosomal cholesterol trafficking	[75]
Wortmannin	Inhibitor of phosphatidylinositol 3-kinase, a lipid kinase implicated in endosomal traffic	[76]
Concanavalin A	Inhibitor of clathrin-mediated endocytosis	[77]

micelles was rapidly converted into the fluorescent agent in serum-containing medium and *in vivo*. These studies are the first to show PCL-b-PEO micelle instability in live animals.

It is generally considered that PEO is ''biocompatible''. However, a number of studies indicate that depending on the cell type, concentration of the polymer or co-polymer used and duration of the cell exposure to PEO, it can induce some damage ([32] reviewed in [89]). We have carried out the experiments to examine cytotoxicity of PCL-b-PEO micelles and found that in relatively low concentrations (<20 μM) they are well tolerated by cells, particularly non-dividing ones or those with long doubling times. In contrast, when a large number of fluorescent dye molecules were non-covalently incorporated into such micelles, cells were damaged. An improved biocompatibility with micelles containing fluorescent dyes was achieved with cross-linked polymer micelles [83].

2. Quantum dots (QDs)

2.1. Photophysics of QDs

Quantum dots (QDs) are colloidal nanocrystals with unique optical properties that make them outstanding fluorescent probes for long-term and multicolor imaging [49,90]. QDs can be excited at single wavelength far removed from their emission maxima, which are tunable by the nanoparticles size. This allows for simultaneous detection of multiple color QDs upon illumination with single light source. QD absorption spectra are broad, but emission spectra are narrow without the red tail characteristic commonly observed with organic dyes. Unlike most organic-based fluorescent dyes, QDs have high resistance towards photobleaching [91]. Electron dense QD core allow their detection by electron microscopy. Combined fluorescence and electron microscopy analyses using the same, multipotent probe provide both the temporal dynamics and high-resolution intracellular localization [92]. Furthermore, QDs have an efficient multiphoton absorption cross-section making them suitable for in vivo imaging [93]. The development of QDs that can emit infrared or near infrared light demonstrated their usefulness for deep tissue imaging [94,95]. Recently, So et al. described the synthesis and use of bioluminescent QD conjugates for *in vivo* imaging [96]. Conjugation of bioluminescent protein to QDs eliminates the need for fluorescent excitation light; instead QDs are excited by bioluminescence resonance energy transfer. Tissue autofluorescence is significantly reduced, and self-illuminating QDs

have greatly enhanced sensitivity in small animal imaging [96].

2.2. QD anatomy

QDs consist of a semiconductor core with or without a passivation shell usually made of ZnS, and additional coatings which are determined by their applications (Fig. 4). The core is made of elements from II–VI (e.g. CdSe, CdTe, CdS, ZnSe), III–V (e.g. InP, InAs) or IV–VI (e.g. PbSe) group, but the most studied QDs in biology are ones with cores made of CdSe or CdTe. The size of the core is 2–10 nm, but the size of the nanoparticles can increase dramatically depending on the coating layer around the core. Thin layer of ZnS on the nanoparticle surface protects the core from oxidation and increases the photoluminescence quantum yield [97]. The surface of nanoparticles is coated with solubilization ligands making QDs water soluble and suitable for use in cell biology [98]. The charge of the nanoparticles is determined by polar groups of the coating ligands and the surrounding pH.

QDs can either be prepared in nonpolar organic solvents yielding nanoparticles non-soluble in water, or they can be prepared by water-based synthesis method. When prepared in organic solvents, their hydrophobic surface ligands are often replaced with hydrophilic ones. A variety of solubilization ligands have been utilized including thiol-containing molecules [99–101], peptides [102], and polymerized silica shells with polar groups [103]. In addition to ligand exchange, nanoparticles with hydrophobic surface ligands can be solubilized by encapsulation in amphiphilic diblock or triblock copolymers [104,105], and in phospholipid micelles [48].

QDs have to be biofunctionalized to act as useful, specific fluorescent labels. Biofunctionalization has been achieved so far by complexation or conjugation of QDs with targeting moieties. The electrostatic interactions between oppositely charged QDs and peptides or proteins have been successfully utilized to specifically label cellular components [106]. QDs with carboxy terminal groups on their surface can be also conjugated to biomolecule amino groups using EDC (1-ethyl-3-(3-dimethylaminopropyl)carbodiimide) as a coupling agent [99,107,108]. Furthermore, modification of QDs can be accomplished by direct binding of thiolated peptides and polyhistidine residues to the QD-surface [109,110]. Since QDs of different colors differ only in the nanoparticle size, the universal approach for conjugation can be applied for labeling with multicolored QDs.

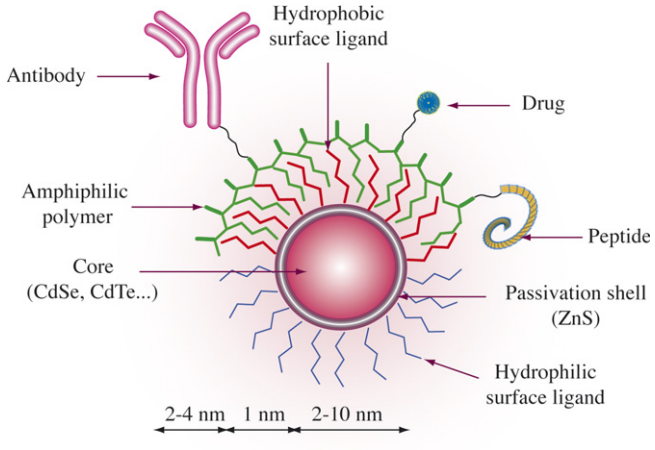

Fig. 4. Anatomy of QDs. Surface modifications of QDs provide protection of the cores and QD targeting. Such modifications considerably enhance QD sizes.

2.3. Internalization and subcellular distribution of QDs

Cellular internalization of QDs can be achieved by different mechanisms including non-specific entry by endocytosis [91], specific entry mediated by biomolecules attached to QD surface [95,99,111], micropipette injection, electroporation, and possibly by inducement of plasma membrane damage [112] (Fig. 5). Without functionalization QDs can enter the cells by endocytosis as shown by colocalization with endosomes/lysosomes using organelle specific dyes [91,107,113]. The mechanism of QD-endocytosis has not been extensively explored and it is not known what endocytotic route they follow. Non-functionalized QDs mainly end up in the cytoplasm and some types of small nanoparticles (green emitting CdTe QDs, coated with cysteamine, 2 nm diameter) can enter the nuclei [108]. The targeting moiety attached to the QD surface determines the mode of entry into cells and their intracellular localization. Selective staining of plasma membrane and intracellular organelles was achieved using QD-labeled antibodies, receptor ligands or targeting peptides. For instance, cancer marker

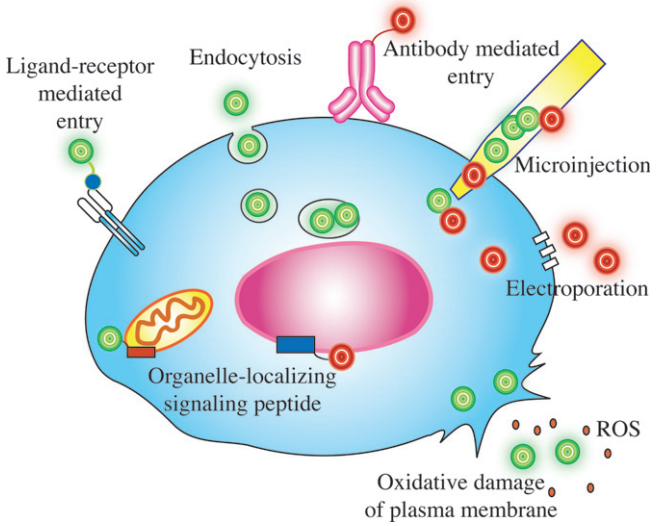

Fig. 5. Internalization of QDs by cells. Cells internalize QDs in different ways depending on cell type, QD concentrations, their sizes, charges or ligands. The extent of internalization of poorly internalized QDs can be enhanced by electroporation and microinjection. Targeting of QDs to different intracellular sites can be achieved by attaching organelle-localizing signal peptides to QD surfaces.

HER2 on the plasma membrane of breast cancer cells was specifically labeled by CdSe/ZnS QDs linked to immunoglobulin G [104]. Streptavidin-coated CdSe/ZnS QDs complexed to biotinylated epidermal growth factor [114] and InP/ZnS QD conjugated to folic acid [115] were internalized by receptor mediated endocytosis. The nucleus was stained by labeling the nuclear antigens with CdSe/ZnS QDs conjugated to antibody, and by linking CdSe/ZnS QDs to nuclear localizing peptide [116].

2.4. Stability of QDs

A crucial role in determining stability of QDs in aqueous environment belongs to the shell and organic molecules attached to the QD surface. Loss of the surface ligands ultimately leads to the precipitation of QDs and loss of their luminescence. Different process can affect stability of surface ligands, and it was shown that the desorption of hydrophilic thiols, common surface ligands used, can be caused by their protonation [117] or by their photooxidation [118]. Deprotonated thiols, thiolates, are bound to cadmium chalcogenide QDs, so if the pH at the QD–ligand interface decreases to a certain value, the ligands get protonated and detach from the QD surface [117]. The precipitation of QDs coated with hydrophilic thiols occurs in a relatively low pH range, between 2 and 7, depending on the size and chemical composition of QDs [117]. It is obvious that the stability and photophysical properties of QDs inside the cells will be strongly dependent on the intracellular localization and the local environment. Photooxidation of surface ligands takes place upon prolonged UV illumination of QDs. Increasing the thickness and packing density of ligand shell can delay initiation process of photooxidation [118]. Preparation of QDs with ligands relatively resistant to photooxidation will enable QDs to fulfill their capacity for long-term cellular or *in vivo* imaging. Due to its inorganic nature, QD core itself is relatively resistant to photodegradation, however, prolonged exposure to UV light affects also the core integrity [118,119].

In summary, the stability and photophysical properties of QDs inside the cells will be strongly dependent on their intracellular localization and its local environment. Conversely, QDs can affect the cell functions, which can be fatal.

2.5. Cytotoxicity of QDs

Both extensively internalized QDs and those that are poorly internalized by cells can eventually cause damage to cellular organelles [108,120]. Biocompatibility of QDs remains a critical issue and a possible limitation to their application especially as *in vivo* diagnostic agents. The unknown interferences of QDs with physiological processes could also lead to misinterpretation of the results in live cell imaging. Obtaining a straight answer about QD cytotoxicity is difficult due to the lack of standardized QD synthesis protocols, coatings, solubilization ligands, and cell systems employed in different studies. However, from this diversity it can be concluded that protection of the QD surface plays a crucial role. Particles with surfaces well protected by polymers or proteins are mostly not harmful to cells [91], whereas breaking down of protective coating (e.g. by irradiation, low lysosomal pH or possibly metabolic degradation) leads to cell damage and death [119]. Two possible mechanisms were proposed to explain this: (i) leaching of metals from the core of nanoparticles with compromised integrity (ions of Cd, Se, Te, Hg, Pb, etc.), and/or (ii) formation of reactive oxygen species (ROS) (Fig. 6). QDs are redox active nanoparticles (effective electron donors and acceptors) [121] and can generate highly reactive free radicals with or without exposure to light [120,122,123]. QDs can induce ROS generation through energy or electron transfer to molecular oxygen [120,122–124]. Cells respond to even small changes of intracellular redox status which is sufficient to inhibit proliferation and induce differentiation [125]. In higher concentrations, ROS are well-known inducers of damage to cellular proteins, lipids, DNA and carbohydrates, and can cause apoptosis or necrosis depending on the severity of damage. Recently, we have provided evidence for the ROS production in live cells incubated with surface-unprotected CdTe QDs [120]. Several fluorescent probes have been used to reveal ROS in live cells: dihydroethidium is used to detect superoxide anion [120,126], Singlet Oxygen Sensor (SOS green) is used for singlet oxygen species and dichlorodihydrofluorescein diacetate detects nearly all ROS nonspecifically. The type of ROS formed strongly depends on the material used to build QDs [127]. When exposed to light QDs are believed to generate singlet oxygen either themselves or due to the molecules conjugated to their surface [122,126]. This property of QDs could be exploited by photodynamic therapy [124].

Toxicity of QDs seems to be also dependent on the charge of the nanoparticles and their ability to form complexes with biomolecules (Fig. 6). Interestingly, even inert polymer coated QDs can exert toxic effects involving several different mechanisms [128].

3. Mechanisms of cell death induced by nanoparticles

A common property of nanoparticles seems to be their ability to induce the generation of ROS [129]. A variety of different nanoparticles, including fullerenes, carbon nanotubes and QDs, were shown to produce ROS *in vitro* [130–132] and *in vivo* [133,134]. Cells are sensitive to ROS and once the production of ROS overcomes the antioxidant defense, cellular redox balance is shifted and the cells are then in a state of oxidative stress. Sensitivity of cells to ROS may depend on the cell type, the level and the duration of oxidant production, the species of ROS generated, and the specific site of ROS production. ROS can react with all types of cellular biomolecules, resulting in their damage, degradation, and finally loss of function [135]. The oxidation of aromatic DNA bases is the main source

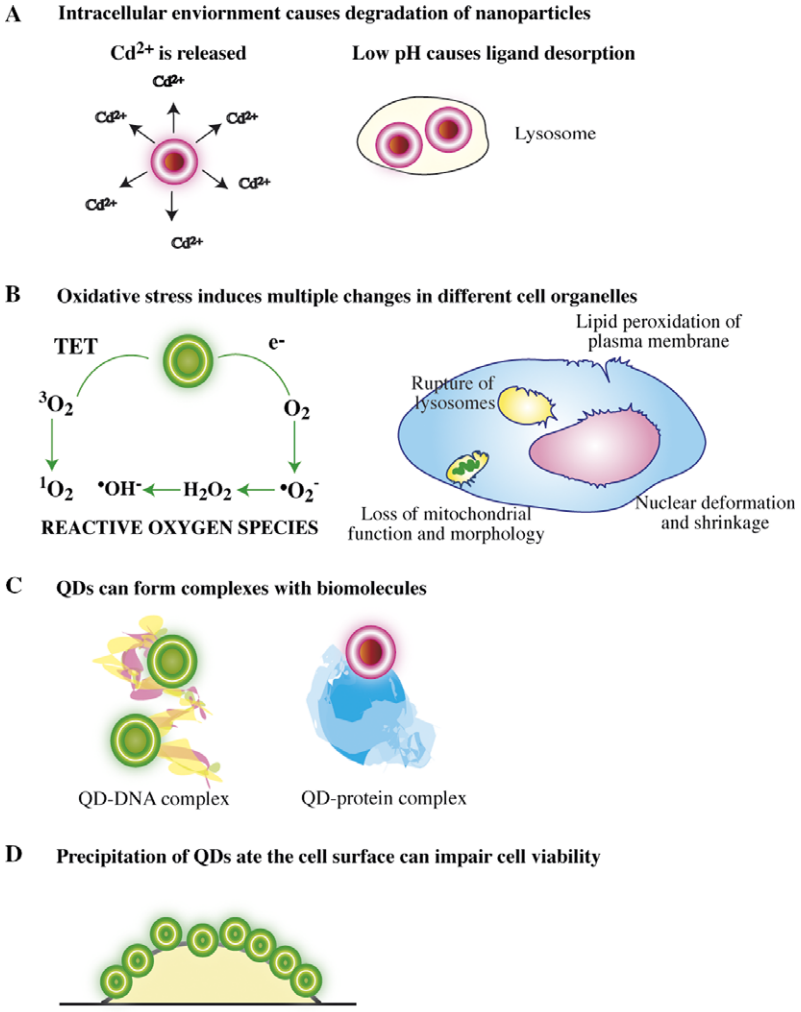

Fig. 6. Interactions between QDs and cells. Stability of QDs will contribute to their interaction with cells. QDs can disintegrate in acidic environment such as lysosomes (A). ROS produced by QDs can induce organelle damage (B). QDs can form complexes with biomolecules (C). Precipitation of QDs at the cell surface even without QD entering the cell can impair cell function and eventually lead to cell death (D) [128].

of DNA damage, while the oxidation of aromatic and sulfur-based amino acids is the main pathway for protein damage. The polyunsaturated fatty acids in lipids are the target for oxidative damage, and their oxidation leads to loss of compartmentalization and plasma-membrane integrity. Moreover, oxidative reactions in membranes lead to amplification of ROS and the formation of bioactive products that influence signaling pathways. Subcellular organelles have their specific redox microenvironment which is controlled by complex antioxidant system that includes antioxidants (glutathione, NADH, thioredoxin) and antioxidant enzymes (superoxide dismutase, catalase, glutathione reductase, and glutathione peroxidase) [136]. Nanoparticles, depending on their subcellular distribution and ROS-producing ability, could induce oxidative damage in certain subcellular organelles and perturb organelle function. Loss of membrane integrity of organelles such as mitochondria or lysosomes results in release of signaling molecules involved in apoptosis. QD-induced oxidative damage to DNA is the most deleterious type of cellular damage often leading to cell death. However, several types of effective coatings and presence of drugs in the cell microenvironment (e.g. *N*-acetylcysteine) significantly enhance QD biocompatibility and minimize cell death even after prolonged exposures [120].

The current high interest in nanobiotechnology and proposed widespread applications of nanoparticles may lead to a mass production of engineered nanoparticles in upcoming years. Humans could become exposed to engineered nanoparticles by inhalation, through the skin, by ingestion or other routes as already shown for environmental ultrafine particles [137]. Understanding nanoparticles – cell interactions and the mechanisms of nanoparticle-induced cytotoxicity are critical factors which address the safety of nanoparticles in science and in our environment.

4. Conclusions

Nanoparticles (micelles and QDs) as drug delivery systems and imaging tools are increasingly employed in

experimental science. Their safety is therefore a prerequisite for their use in medicine. Novel approaches which provide biocompatible drug nanocarriers and luminescent biomarkers (e.g. those that emit in the near infrared region or responding to different intracellular stimuli) are gaining momentum in the development of future diagnostics and therapeutics.

Acknowledgement

The authors acknowledge the support by the Canadian Institutes (CIHR) for Health Research and Juvenile Diabetes Research Foundation (JDRF).

References

[1] M.L. Adams, A. Lavasanifar, G.S. Kwon, Amphiphilic block copolymers for drug delivery, J. Pharm. Sci. 92 (2003) 1343–1355.
[2] W.R. Gombotz, G.H. Wang, T.A. Horbett, A.S. Hoffman, Protein adsorption to poly(ethylene oxide) surfaces, J. Biomed. Mater. Res. 25 (1991) 1547–1562.
[3] S. Stolnik, B. Daudali, A. Arien, J. Whetstone, C.R. Heald, M.C. Garnett, S.S. Davis, L. Illum, The effect of surface coverage and conformation of poly(ethylene oxide) (PEO) chains of poloxamer 407 on the biological fate of model colloidal drug carriers, Biochim. Biophys. Acta 1514 (2001) 261–279.
[4] I. Szleifer, Polymers and proteins: interactions at interfaces, Curr. Opin. Solid State Mater. Sci. 2 (1997) 337–344.
[5] D.E. Discher, A. Eisenberg, Polymer vesicles, Science 297 (2002) 967–973.
[6] A. Choucair, A. Eisenberg, Control of amphiphilic block copolymer morphologies using solution conditions, Eur. Phys. J. E Soft Matter 10 (2003) 37–44.
[7] L. Zhang, K. Yu, A. Eisenberg, Ion-induced morphological changes in "Crew-Cut" aggregates of amphiphilic block copolymers, Science 272 (1996) 1777–1779.
[8] C. Allen, D. Maysinger, A. Eisenberg, Nano-engineering block copolymer aggregates for drug delivery, Colloids Surf. B Biointerfaces 16 (1999) 3–27.
[9] G.S. Kwon, Polymeric micelles for delivery of poorly water-soluble compounds, Crit. Rev. Ther. Drug Carrier Syst 20 (2003) 357–403.
[10] H. Maeda, Y. Matsumura, Tumoritropic and lymphotropic principles of macromolecular drugs, Crit. Rev. Ther. Drug Carrier Syst. 6 (1989) 193–210.
[11] R. Duncan, The dawning era of polymer therapeutics, Nat. Rev. Drug Discov. 2 (2003) 347–360.
[12] T.Y. Kim, D.W. Kim, J.Y. Chung, S.G. Shin, S.C. Kim, D.S. Heo, N.K. Kim, Y.J. Bang, Phase I and pharmacokinetic study of Genexol-PM, a cremophor-free, polymeric micelle-formulated paclitaxel, in patients with advanced malignancies, Clin. Cancer Res. 10 (2004) 3708–3716.
[13] Y. Matsumura, T. Hamaguchi, T. Ura, K. Muro, Y. Yamada, Y. Shimada, K. Shirao, T. Okusaka, H. Ueno, M. Ikeda, N. Watanabe, Phase I clinical trial and pharmacokinetic evaluation of NK911, a micelle-encapsulated doxorubicin, Br. J. Cancer 91 (2004) 1775–1781.
[14] T. Hamaguchi, Y. Matsumura, M. Suzuki, K. Shimizu, R. Goda, I. Nakamura, I. Nakatomi, M. Yokoyama, K. Kataoka, T. Kakizoe, NK105, a paclitaxel-incorporating micellar nanoparticle formulation, can extend in vivo antitumour activity and reduce the neurotoxicity of paclitaxel, Br. J. Cancer 92 (2005) 1240–1246.
[15] P. Lim Soo, J. Lovric, P. Davidson, D. Maysinger, A. Eisenberg, Polycaprolactone-block-poly(ethylene oxide) micelles: a nanodelivery system for 17beta-estradiol, Mol. Pharm. 2 (2005) 519–527.
[16] C. Allen, J. Han, Y. Yu, D. Maysinger, A. Eisenberg, Polycaprolactone-b-poly(ethylene oxide) copolymer micelles as a delivery vehicle for dihydrotestosterone, J. Control. Release 63 (2000) 275–286.
[17] C. Allen, A. Eisenberg, J. Mrsic, D. Maysinger, PCL-b-PEO micelles as a delivery vehicle for FK506: assessment of a functional recovery of crushed peripheral nerve, Drug Deliv. 7 (2000) 139–145.
[18] K. Novakova, M. Laznicek, F. Rypacek, L. Machova, Pharmacokinetics and distribution of 125I-PLA-b-PEO block copolymers in rats, Pharm. Dev. Technol. 8 (2003) 153–161.
[19] A. Benahmed, M. Ranger, J.C. Leroux, Novel polymeric micelles based on the amphiphilic diblock copolymer poly(*N*-vinyl-2-pyrrolidone)-block-poly(D,L-lactide), Pharm. Res. 18 (2001) 323–328.
[20] A.K. Gupta, S. Madan, D.K. Majumdar, A. Maitra, Ketorolac entrapped in polymeric micelles: preparation, characterisation and ocular anti-inflammatory studies, Int. J. Pharm. 209 (2000) 1–14.
[21] Y. Kakizawa, K. Kataoka, Block copolymer micelles for delivery of gene and related compounds, Adv. Drug Deliv. Rev. 54 (2002) 203–222.
[22] A.V. Kabanov, E.V. Batrakova, S. Sriadibhatla, Z. Yang, D.L. Kelly, V.Y. Alakov, Polymer genomics: shifting the gene and drug delivery paradigms, J. Control. Release 101 (2005) 259–271.
[23] G. Gaucher, M.H. Dufresne, V.P. Sant, N. Kang, D. Maysinger, J.C. Leroux, Block copolymer micelles: preparation, characterization and application in drug delivery, J. Control. Release 109 (2005) 169–188.
[24] D. Wakebayashi, N. Nishiyama, Y. Yamasaki, K. Itaka, N. Kanayama, A. Harada, Y. Nagasaki, K. Kataoka, Lactose-conjugated polyion complex micelles incorporating plasmid DNA as a targetable gene vector system: their preparation and gene transfecting efficiency against cultured HepG2 cells, J. Control. Release 95 (2004) 653–664.
[25] M. Oishi, S. Sasaki, Y. Nagasaki, K. Kataoka, pH-responsive oligodeoxynucleotide (ODN)-poly(ethylene glycol) conjugate through acid-labile beta-thiopropionate linkage: preparation and polyion complex micelle formation, Biomacromolecules 4 (2003) 1426–1432.
[26] A. Harada, K. Kataoka, Pronounced activity of enzymes through the incorporation into the core of polyion complex micelles made from charged block copolymers, J. Control. Release 72 (2001) 85–91.
[27] M.H. Dufresne, J.C. Leroux, Study of the micellization behavior of different order amino block copolymers with heparin, Pharm. Res. 21 (2004) 160–169.
[28] T. Govender, S. Stolnik, C. Xiong, S. Zhang, L. Illum, S.S. Davis, Drug-polyionic block copolymer interactions for micelle formation: physicochemical characterisation, J. Control. Release 75 (2001) 249–258.
[29] L. Luo, J. Tam, D. Maysinger, A. Eisenberg, Cellular internalization of poly(ethylene oxide)-b-poly(epsilon-caprolactone) diblock copolymer micelles, Bioconjug. Chem. 13 (2002) 1259–1265.
[30] N. Rapoport, A. Marin, Y. Luo, G.D. Prestwich, M.D. Muniruzzaman, Intracellular uptake and trafficking of Pluronic micelles in drug-sensitive and MDR cells: effect on the intracellular drug localization, J. Pharm. Sci. 91 (2002) 157–170.
[31] H.S. Yoo, T.G. Park, Folate-receptor-targeted delivery of doxorubicin nano-aggregates stabilized by doxorubicin–PEG–folate conjugate, J. Control. Release 100 (2004) 247–256.
[32] R. Savic, L. Luo, A. Eisenberg, D. Maysinger, Micellar nanocontainers distribute to defined cytoplasmic organelles, Science 300 (2003) 615–618.
[33] L. Araujo, R. Lobenberg, J. Kreuter, Influence of the surfactant concentration on the body distribution of nanoparticles, J Drug Target 6 (1999) 373–385.
[34] E.V. Batrakova, S. Li, Y. Li, V.Y. Alakhov, W.F. Elmquist, A.V. Kabanov, Distribution kinetics of a micelle-forming block copolymer Pluronic P85, J. Control. Release 100 (2004) 389–397.
[35] R.C. Jewell, S.P. Khor, D.F. Kisor, K.A. LaCroix, W.A. Wargin, Pharmacokinetics of RheothRx injection in healthy male volunteers, J. Pharm. Sci. 86 (1997) 808–812.

[36] S.N. Sidorov, L.M. Bronstein, Y.A. Kabachii, P.M. Valetsky, P.L. Soo, D. Maysinger, A. Eisenberg, Influence of metalation on the morphologies of poly(ethylene oxide)-block-poly(4-vinylpyridine) block copolymer micelles, Langmuir 20 (2004) 3543–3550.
[37] T. Sakai, P. Alexandridis, Single-step synthesis and stabilization of metal nanoparticles in aqueous pluronic block copolymer solutions at ambient temperature, Langmuir 20 (2004) 8426–8430.
[38] H. Otsuka, Y. Akiyama, Y. Nagasaki, K. Kataoka, Quantitative and reversible lectin-induced association of gold nanoparticles modified with alpha-lactosyl-omega-mercapto-poly(ethylene glycol), J. Am. Chem. Soc. 123 (2001) 8226–8230.
[39] Y. Sun, Y. Xia, Shape-controlled synthesis of gold and silver nanoparticles, Science 298 (2002) 2176–2179.
[40] K. Kamata, Y. Lu, Y. Xia, Synthesis and characterization of monodispersed core-shell spherical colloids with movable cores, J. Am. Chem. Soc. 125 (2003) 2384–2385.
[41] M.K. Corbierre, N.S. Cameron, M. Sutton, S.G. Mochrie, L.B. Lurio, A. Ruhm, R.B. Lennox, Polymer-stabilized gold nanoparticles and their incorporation into polymer matrices, J. Am. Chem. Soc. 123 (2001) 10411–10412.
[42] K. Ohno, K.-m. Koh, Y. Tsujii, T. Fukuda, Synthesis of gold nanoparticles coated with well-defined, high-density polymer brushes by surface-initiated living radical polymerization, Macromolecules (2002) 8989–8993.
[43] S.M. Marinakos, J.P. Novak, L.C. Brousseau, A. Blaine House, E.M. Edeki, J.C. Feldhaus, D.L. Feldheim, Gold particles as templates for the synthesis of hollow polymer capsules. Control of capsule dimensions and guest encapsulation, J. Am. Chem. Soc. 121 (1999) 8518–8522.
[44] R. Savic, D. Maysinger, Intracellular fate of block copolymer micelles, Control. Release Soc. Newslett. 21 (2004) 7.
[45] M. Peter, S.M. Ameer-Beg, Imaging molecular interactions by multiphoton FLIM, Biol. Cell 96 (2004) 231–236.
[46] M. Wahl, F. Koberling, M. Patting, H. Rahn, R. Erdmann, Time-resolved confocal fluorescence imaging and spectroscopy system with single molecule sensitivity and sub-micrometer resolution, Curr. Pharm. Biotechnol. 5 (2004) 299–308.
[47] P.I. Bastiaens, A. Squire, Fluorescence lifetime imaging microscopy: spatial resolution of biochemical processes in the cell, Trends Cell Biol. 9 (1999) 48–52.
[48] B. Dubertret, P. Skourides, D.J. Norris, V. Noireaux, A.H. Brivanlou, A. Libchaber, In vivo imaging of quantum dots encapsulated in phospholipid micelles, Science 298 (2002) 1759–1762.
[49] I.L. Medintz, H.T. Uyeda, E.R. Goldman, H. Mattoussi, Quantum dot bioconjugates for imaging, labelling and sensing, Nat. Mater. 4 (2005) 435–446.
[50] N. Duxin, F. Liu, H. Vali, A. Eisenberg, Cadmium sulphide quantum dots in morphologically tunable triblock copolymer aggregates, J. Am. Chem. Soc. 127 (2005) 10063–10069.
[51] C.J. Merrifield, M.E. Feldman, L. Wan, W. Almers, Imaging actin and dynamin recruitment during invagination of single clathrin-coated pits, Nat Cell Biol. 4 (2002) 691–698.
[52] F.T. Mu, J.M. Callaghan, O. Steele-Mortimer, H. Stenmark, R.G. Parton, P.L. Campbell, J. McCluskey, J.P. Yeo, E.P. Tock, B.H. Toh, EEA1, an early endosome-associated protein. EEA1 is a conserved alpha-helical peripheral membrane protein flanked by cysteine "fingers" and contains a calmodulin-binding IQ motif, J. Biol. Chem. 270 (1995) 13503–13511.
[53] R.E. Harrison, C. Bucci, O.V. Vieira, T.A. Schroer, S. Grinstein, Phagosomes fuse with late endosomes and/or lysosomes by extension of membrane protrusions along microtubules: role of Rab7 and RILP, Mol. Cell Biol. 23 (2003) 6494–6506.
[54] J. Rejman, V. Oberle, I.S. Zuhorn, D. Hoekstra, Size-dependent internalization of particles via the pathways of clathrin- and caveolae-mediated endocytosis, Biochem. J. 377 (2004) 159–169.
[55] H. Bannai, T. Inoue, T. Nakayama, M. Hattori, K. Mikoshiba, Kinesin dependent, rapid, bi-directional transport of ER sub-compartment in dendrites of hippocampal neurons, J. Cell Sci. 117 (2004) 163–175.
[56] O. Shupliakov, O. Bloom, J.S. Gustafsson, O. Kjaerulff, P. Low, N. Tomilin, V.A. Pieribone, P. Greengard, L. Brodin, Impaired recycling of synaptic vesicles after acute perturbation of the presynaptic actin cytoskeleton, Proc. Natl. Acad. Sci. USA 99 (2002) 14476–14481.
[57] S. Mukherjee, R.N. Ghosh, F.R. Maxfield, Endocytosis, Physiol. Rev. 77 (1997) 759–803.
[58] S.D. Conner, S.L. Schmid, Regulated portals of entry into the cell, Nature 422 (2003) 37–44.
[59] M.J. Clague, Molecular aspects of the endocytic pathway, Biochem. J. 336 (Pt 2) (1998) 271–282.
[60] A.M. van der Bliek, T.E. Redelmeier, H. Damke, E.J. Tisdale, E.M. Meyerowitz, S.L. Schmid, Mutations in human dynamin block an intermediate stage in coated vesicle formation, J. Cell Biol. 122 (1993) 553–563.
[61] B. Zhang, Y.H. Koh, R.B. Beckstead, V. Budnik, B. Ganetzky, H.J. Bellen, Synaptic vesicle size and number are regulated by a clathrin adaptor protein required for endocytosis, Neuron 21 (1998) 1465–1475.
[62] A. Benmerah, M. Bayrou, N. Cerf-Bensussan, A. Dautry-Varsat, Inhibition of clathrin-coated pit assembly by an Eps15 mutant, J. Cell Sci. 112 (Pt 9) (1999) 1303–1311.
[63] C. Bucci, R.G. Parton, I.H. Mather, H. Stunnenberg, K. Simons, B. Hoflack, M. Zerial, The small GTPase rab5 functions as a regulatory factor in the early endocytic pathway, Cell 70 (1992) 715–728.
[64] Y. Feng, B. Press, A. Wandinger-Ness, Rab 7: an important regulator of late endocytic membrane traffic, J. Cell Biol. 131 (1995) 1435–1452.
[65] C. D'Souza-Schorey, G. Li, M.I. Colombo, P.D. Stahl, A regulatory role for ARF6 in receptor-mediated endocytosis, Science 267 (1995) 1175–1178.
[66] C. Lamaze, T.H. Chuang, L.J. Terlecky, G.M. Bokoch, S.L. Schmid, Regulation of receptor-mediated endocytosis by Rho and Rac, Nature 382 (1996) 177–179.
[67] B. Qualmann, H. Mellor, Regulation of endocytic traffic by Rho GTPases, Biochem. J. 371 (2003) 233–241.
[68] N.K. Hussain, S. Jenna, M. Glogauer, C.C. Quinn, S. Wasiak, M. Guipponi, S.E. Antonarakis, B.K. Kay, T.P. Stossel, N. Lamarche-Vane, P.S. McPherson, Endocytic protein intersectin-l regulates actin assembly via Cdc42 and N-WASP, Nat. Cell Biol. 3 (2001) 927–932.
[69] M. Drab, P. Verkade, M. Elger, M. Kasper, M. Lohn, B. Lauterbach, J. Menne, C. Lindschau, F. Mende, F.C. Luft, A. Schedl, H. Haller, T.V. Kurzchalia, Loss of caveolae, vascular dysfunction, and pulmonary defects in caveolin-1 gene-disrupted mice, Science 293 (2001) 2449–2452.
[70] J.R. Peterson, T.J. Mitchison, Small molecules, big impact: a history of chemical inhibitors and the cytoskeleton, Chem. Biol. 9 (2002) 1275–1285.
[71] M. Coue, S.L. Brenner, I. Spector, E.D. Korn, Inhibition of actin polymerization by latrunculin A, FEBS Lett. 213 (1987) 316–318.
[72] H.H. Mollenhauer, D.J. Morre, L.D. Rowe, Alteration of intracellular traffic by monensin; mechanism, specificity and relationship to toxicity, Biochim. Biophys. Acta 1031 (1990) 225–246.
[73] A.M. Tartakoff, Perturbation of vesicular traffic with the carboxylic ionophore monensin, Cell 32 (1983) 1026–1028.
[74] R.D. Klausner, J.G. Donaldson, J. Lippincott-Schwartz, Brefeldin A: insights into the control of membrane traffic and organelle structure, J. Cell Biol. 116 (1992) 1071–1080.
[75] L.S. Johnson, K.W. Dunn, B. Pytowski, T.E. McGraw, Endosome acidification and receptor trafficking: bafilomycin A1 slows receptor externalization by a mechanism involving the receptor's internalization motif, Mol. Biol. Cell 4 (1993) 1251–1266.
[76] H. Shpetner, M. Joly, D. Hartley, S. Corvera, Potential sites of PI-3 kinase function in the endocytic pathway revealed by the PI-3 kinase inhibitor, wortmannin, J. Cell Biol. 132 (1996) 595–605.

[77] S. Drose, K. Altendorf, Bafilomycins and concanamycins as inhibitors of V-ATPases and P-ATPases, J. Exp. Biol. 200 (1997) 1–8.
[78] K.K. Jette, D. Law, E.A. Schmitt, G.S. Kwon, Preparation and drug loading of poly(ethylene glycol)-block-poly(epsilon-caprolactone) micelles through the evaporation of a cosolvent azeotrope, Pharm Res. 21 (2004) 1184–1191.
[79] M. Ranger, M.C. Jones, M.A. Yessine, J.C. Leroux, From well-defined diblock copolymers prepared by a versatile atom transfer radical polymerization method to supramolecular assemblies, J. Polymer Sci. Part A-Polymer Chem. 39 (2001).
[80] M.L. Adams, D.R. Andes, G.S. Kwon, Amphotericin B encapsulated in micelles based on poly(ethylene oxide)-block-poly(L-amino acid) derivatives exerts reduced in vitro hemolysis but maintains potent in vivo antifungal activity, Biomacromolecules 4 (2003) 750–757.
[81] M.L. Adams, G.S. Kwon, Relative aggregation state and hemolytic activity of amphotericin B encapsulated by poly(ethylene oxide)-block-poly(*N*-hexyl-L-aspartamide)-acyl conjugate micelles: effects of acyl chain length, J. Control. Release 87 (2003) 23–32.
[82] Y. Yamamoto, K. Yasugi, A. Harada, Y. Nagasaki, K. Kataoka, Temperature-related change in the properties relevant to drug delivery of poly(ethylene glycol)-poly(D,L-lactide) block copolymer micelles in aqueous milieu, J. Control. Release 82 (2002) 359–371.
[83] K.B. Thurmond, H.Y. Huang, C.G. Clark, T. Kowalewski, K.L. Wooley, Shell cross-linked polymer micelles: stabilized assemblies with great versatility and potential, Colloids Surf. B Biointerfaces 16 (1999) 45–54.
[84] X. Shuai, T. Merdan, A.K. Schaper, F. Xi, T. Kissel, Core-cross-linked polymeric micelles as paclitaxel carriers, Bioconjug. Chem. 15 (2004) 441–448.
[85] M. Jaturanpinyo, A. Harada, X. Yuan, K. Kataoka, Preparation of bionanoreactor based on core-shell structured polyion complex micelles entrapping trypsin in the core cross-linked with glutaraldehyde, Bioconjug. Chem. 15 (2004) 344–348.
[86] J. Lee, E.C. Cho, K. Cho, Incorporation and release behavior of hydrophobic drug in functionalized poly(D,L-lactide)-block-poly(ethylene oxide) micelles, J. Control. Release 94 (2004) 323–335.
[87] A. Harada, H. Togawa, K. Kataoka, Physicochemical properties and nuclease resistance of antisense-oligodeoxynucleotides entrapped in the core of polyion complex micelles composed of poly(ethylene glycol)-poly(L-lysine) block copolymers, Eur. J. Pharm. Sci. 13 (2001) 35–42.
[88] R. Savic, T. Azzam, A. Eisenberg, D. Maysinger, Assessment of the integrity of poly(caprolactone)-b-poly(ethylene oxide) micelles under biological conditions: a fluorogenic-based approach, Langmuir 22 (2006) 3570–3578.
[89] S.M. Moghimi, A.C. Hunter, J.C. Murray, Nanomedicine: current status and future prospects, Faseb J. 19 (2005) 311–330.
[90] X. Michalet, F.F. Pinaud, L.A. Bentolila, J.M. Tsay, S. Doose, J.J. Li, G. Sundaresan, A.M. Wu, S.S. Gambhir, S. Weiss, Quantum dots for live cells, in vivo imaging, and diagnostics, Science 307 (2005) 538–544.
[91] J.K. Jaiswal, H. Mattoussi, J.M. Mauro, S.M. Simon, Long-term multiple color imaging of live cells using quantum dot bioconjugates, Nat. Biotechnol. 21 (2003) 47–51.
[92] M. Dahan, S. Levi, C. Luccardini, P. Rostaing, B. Riveau, A. Triller, Diffusion dynamics of glycine receptors revealed by single-quantum dot tracking, Science 302 (2003) 442–445.
[93] D.R. Larson, W.R. Zipfel, R.M. Williams, S.W. Clark, M.P. Bruchez, F.W. Wise, W.W. Webb, Water-soluble quantum dots for multiphoton fluorescence imaging in vivo, Science 300 (2003) 1434–1436.
[94] S. Kim, Y.T. Lim, E.G. Soltesz, A.M. De Grand, J. Lee, A. Nakayama, J.A. Parker, T. Mihaljevic, R.G. Laurence, D.M. Dor, L.H. Cohn, M.G. Bawendi, J.V. Frangioni, Near-infrared fluorescent type II quantum dots for sentinel lymph node mapping, Nat. Biotechnol. 22 (2004) 93–97.
[95] E.B. Voura, J.K. Jaiswal, H. Mattoussi, S.M. Simon, Tracking metastatic tumor cell extravasation with quantum dot nanocrystals and fluorescence emission-scanning microscopy, Nat. Med. 10 (2004) 993–998.
[96] M.K. So, C. Xu, A.M. Loening, S.S. Gambhir, J. Rao, Self-illuminating quantum dot conjugates for in vivo imaging, Nat. Biotechnol. 24 (2006) 339–343.
[97] B.O. Dabbousi, J. Rodriguez-Viejo, F.V. Mikulec, J.R. Heine, H. Mattoussi, R. Ober, K.F. Jensen, M.G. Bawendu, (CdSe)ZnS core shell quantum dots: synthesis and characterization of a size series of highly luminescent nanocrystallites, J. Phys. Chem. B 101 (1997) 9463–9475.
[98] C. Seydel, Quantum dots get wet, Science 300 (2003) 80–81.
[99] W.C. Chan, S. Nie, Quantum dot bioconjugates for ultrasensitive nonisotopic detection, Science 281 (1998) 2016–2018.
[100] S. Pathak, S.K. Choi, N. Arnheim, M.E. Thompson, Hydroxylated quantum dots as luminescent probes for in situ hybridization, J. Am. Chem. Soc. 123 (2001) 4103–4104.
[101] N. Gaponik, D.V. Talapin, A.L. Rogach, K. Hoppe, E.V. Shevchenko, A. Kornowski, A. Eychmuller, H. Weller, Thiol-capping of CdTe nanocrystals: an alternative to organometallic synthetic routes, J. Phys. Chem. B 106 (2002) 7177–7185.
[102] F. Pinaud, D. King, H.P. Moore, S. Weiss, Bioactivation and cell targeting of semiconductor CdSe/ZnS nanocrystals with phytochelatin-related peptides, J. Am. Chem. Soc. 126 (2004) 6115–6123.
[103] M. Bruchez Jr., M. Moronne, P. Gin, S. Weiss, A.P. Alivisatos, Semiconductor nanocrystals as fluorescent biological labels, Science 281 (1998) 2013–2016.
[104] X. Wu, H. Liu, J. Liu, K.N. Haley, J.A. Treadway, J.P. Larson, N. Ge, F. Peale, M.P. Bruchez, Immunofluorescent labeling of cancer marker Her2 and other cellular targets with semiconductor quantum dots, Nat. Biotechnol. 21 (2003) 41–46.
[105] X. Gao, Y. Cui, R.M. Levenson, L.W. Chung, S. Nie, In vivo cancer targeting and imaging with semiconductor quantum dots, Nat. Biotechnol. 22 (2004) 969–976.
[106] K. Hanaki, A. Momo, T. Oku, A. Komoto, S. Maenosono, Y. Yamaguchi, K. Yamamoto, Semiconductor quantum dot/albumin complex is a long-life and highly photostable endosome marker, Biochem. Biophys. Res. Commun. 302 (2003) 496–501.
[107] A.M. Derfus, W.C.W. Chan, S.N. Bhatia, Intracellular delivery of quantum dots for live cell labeling and organelle tracking, Adv. Mater. 16 (2004) 961–966.
[108] J. Lovric, H.S. Bazzi, Y. Cuie, G.R. Fortin, F.M. Winnik, D. Maysinger, Differences in subcellular distribution and toxicity of green and red emitting CdTe quantum dots, J. Mol. Med. 83 (2005) 377–385.
[109] M.E. Akerman, W.C. Chan, P. Laakkonen, S.N. Bhatia, E. Ruoslahti, Nanocrystal targeting in vivo, Proc. Natl. Acad. Sci. USA 99 (2002) 12617–12621.
[110] J.M. Slocik, J.T. Moore, D.W. Wright, Monoclonal antibody recognition of histidine-rich peptide encapsulated nanoclusters, NanoLetters 2 (2002) 169–173.
[111] F. Chen, D. Gerion, Fluorescent CdSe/ZnS nanocrystal-peptide conjugates for long-term, nontoxic imaging and nuclear targeting in living cells, NanoLetters 4 (2004) 1827–1832.
[112] J.A. Kloepfer, R.E. Mielke, J.L. Nadeau, Uptake of CdSe and CdSe/ZnS quantum dots into bacteria via purine-dependent mechanisms, Appl. Environ. Microbiol. 71 (2005) 2548–2557.
[113] W.J. Parak, R. Boudreau, M. Le Gros, D. Gerion, D. Zanchet, C.M. Micheel, S.C. Williams, A.P. Alivisatos, C. Larabell, Cell motility and metastatic potential studies based on quantum dot imaging of phagokinetic tracks, Adv. Mater. 14 (2002) 882–885.
[114] D.S. Lidke, P. Nagy, R. Heintzmann, D.J. Arndt-Jovin, J.N. Post, H.E. Grecco, E.A. Jares-Erijman, T.M. Jovin, Quantum dot ligands provide new insights into erbB/HER receptor-mediated signal transduction, Nat. Biotechnol. 22 (2004) 198–203.
[115] D.J. Bharali, D.W. Lucey, H. Jayakumar, H.E. Pudavar, P.N. Prasad, Folate-receptor-mediated delivery of InP quantum dots for

bioimaging using confocal and two-photon microscopy, J. Am. Chem. Soc. 127 (2005) 11364–11371.
[116] A. Hoshino, K. Fujioka, T. Oku, S. Nakamura, M. Suga, Y. Yamaguchi, K. Suzuki, M. Yasuhara, K. Yamamoto, Quantum dots targeted to the assigned organelle in living cells, Microbiol. Immunol. 48 (2004) 985–994.
[117] J. Aldana, N. Lavelle, Y. Wang, X. Peng, Size-dependent dissociation pH of thiolate ligands from cadmium chalcogenide nanocrystals, J. Am. Chem. Soc. 127 (2005) 2496–2504.
[118] J. Aldana, Y.A. Wang, X. Peng, Photochemical instability of CdSe nanocrystals coated by hydrophilic thiols, J. Am. Chem. Soc. 123 (2001) 8844–8850.
[119] A. Derfus, W. Chen, S. Bhatia, Probin the cytotoxicity of semiconductor quantum dots, NanoLetters 4 (2004) 11–18.
[120] J. Lovric, S.J. Cho, F.M. Winnik, D. Maysinger, Unmodified cadmium telluride quantum dots induce reactive oxygen species formation leading to multiple organelle damage and cell death, Chem. Biol. 12 (2005) 1227–1234.
[121] S.K. Haram, B.M. Quinn, A.J. Bard, Electrochemistry of CdS nanoparticles: a correlation between optical and electrochemical band gaps, J. Am. Chem. Soc. 123 (2001) 8860–8861.
[122] A.C. Samia, X. Chen, C. Burda, Semiconductor quantum dots for photodynamic therapy, J. Am. Chem. Soc. 125 (2003) 15736–15737.
[123] M. Green, E. Howman, Semiconductor quantum dots and free radical induced DNA nicking, Chem. Commun. (Camb) (2005) 121–123.
[124] R. Bakalova, H. Ohba, Z. Zhelev, M. Ishikawa, Y. Baba, Quantum dots as photosensitizers? Nat. Biotechnol. 22 (2004) 1360–1361.
[125] M. Noble, M. Mayer-Proschel, C. Proschel, Redox regulation of precursor cell function: insights and paradoxes, Antioxid. Redox Signal. 7 (2005) 1456–1467.
[126] S.J. Clarke, C.A. Hollmann, Z. Zhang, D. Suffern, S.E. Bradforth, N.M. Dimitrijevic, W.G. Minarik, J.L. Nadeau, Photophysics of dopamine-modified quantum dots and effects on biological systems, Nat. Mater. (2006).
[127] B.I. Ipe, M. Lehnig, C.M. Niemeyer, On the generation of free radical species from quantum dots, Small 1 (2005) 706–709.
[128] C. Kirchner, T. Liedl, S. Kudera, T. Pellegrino, A. Munoz Javier, H.E. Gaub, S. Stolzle, N. Fertig, W.J. Parak, Cytotoxicity of colloidal CdSe and CdSe/ZnS nanoparticles, NanoLetters 5 (2005) 331–338.
[129] A. Nel, T. Xia, L. Madler, N. Li, Toxic potential of materials at the nanolevel, Science 311 (2006) 622–627.
[130] Y. Yamakoshi, N. Umezawa, A. Ryu, K. Arakane, N. Miyata, Y. Goda, T. Masumizu, T. Nagano, Active oxygen species generated from photoexcited fullerene (C60) as potential medicines: O2-* versus 1O2, J. Am. Chem. Soc. 125 (2003) 12803–12809.
[131] K.D. Pickering, M.R. Wiesner, Fullerol-sensitized production of reactive oxygen species in aqueous solution, Environ. Sci. Technol. 39 (2005) 1359–1365.
[132] A.A. Shvedova, V. Castranova, E.R. Kisin, D. Schwegler-Berry, A.R. Murray, V.Z. Gandelsman, A. Maynard, P. Baron, Exposure to carbon nanotube material: assessment of nanotube cytotoxicity using human keratinocyte cells, J. Toxicol. Environ. Health A 66 (2003) 1909–1926.
[133] E. Oberdorster, Manufactured nanomaterials (fullerenes, C60) induce oxidative stress in the brain of juvenile largemouth bass, Environ. Health Perspect. 112 (2004) 1058–1062.
[134] J.P. Kamat, T.P. Devasagayam, K.I. Priyadarsini, H. Mohan, Reactive oxygen species mediated membrane damage induced by fullerene derivatives and its possible biological implications, Toxicology 155 (2000) 55–61.
[135] B. Halliwell, J.M.C. Gutteridge, Free Radicals in Biology and Medicine, III, Oxford University Press, New York, 1999.
[136] L. Moldovan, N.I. Moldovan, Oxygen free radicals and redox biology of organelles, Histochem. Cell Biol. 122 (2004) 395–412.
[137] G. Oberdorster, E. Oberdorster, J. Oberdorster, Nanotoxicology: an emerging discipline evolving from studies of ultrafine particles, Environ. Health Perspect. 113 (2005) 823–839.